Conformerism, enantiomorphism and double catemer motifs in *para*-substituted nostoclide analogues

Róbson Ricardo Teixeira [a, b], Luiz Claudio Almeida Barbosa [a, b, *], Isabel Valero Antolinez [a], Rodrigo de Souza Corrêa [d], Felipe Terra Martins [e, **], Antônio Carlos Doriguetto [c, ***]

[a] Chemistry Department, Universidade Federal de Minas Gerais, CEP 3409-5720 Belo Horizonte, MG, Brazil
[b] Chemistry Department, Universidade Federal de Viçosa, CEP 36570-900 Viçosa, MG, Brazil
[c] Institute of Chemistry, Federal University of Alfenas, CEP 37130-000 Alfenas, MG, Brazil
[d] Chemistry Department, Federal University of OuroPreto, CEP 35400-000 OuroPreto, MG, Brazil
[e] Chemical Institute, Federal University of Goiás, CEP 74001-970 Goiânia, GO, Brazil

A B S T R A C T

We have here elucidated the crystal structures of five nostoclide analogues. A common feature in all compounds is a substituent at the *para*-position of the benzylidene group. Compounds with either bromine (**3**) or hydroxyl (**4**) as *para*-substituent crystallizes with Z' = 2 as result of conformerism. It was also observed that Z' > 1 in the compound with a *para*-dimethylamino substituent (**1**). However, its four crystallographically independent molecules are conformationally similar. They are not related by crystallographic symmetry due to the offset packing of their C−H ⋯ O=C nonclassical hydrogen bonded double chains. This compound (**1**) has also crystallized in a chiral space group (P2₁) despite the lack of a stereocenter. Such enantiomorphism phenomenon is related to the presence of only one of the two mirror benzyl conformations with phenyl ring at the equatorial position opposite the lactone oxygen atom. The molecular mean plane of nostoclide analogues has been featured by high level of planarity, except in the brominated compound where two twisted conformations occurred due to rotations on the single bond axis into benzylidene group. The benzyl conformation has been the greatest difference between the two crystallographically independent molecules of the *para*-hydroxylated compound (**4**). The crystal packing of the compounds is marked by double catemer motif assembled through C−H ⋯ O= C non-classical hydrogen bonds, although C−H ⋯ π interactions do play an important role in stabilizing the crystal packing of some compounds of the series.

© 2015 Elsevier B.V. All rights reserved.

1. Introduction

The exploitation of marine species as source of natural products has been rewarding. A plethora of compounds of various complexities has been isolated from marine microorganisms and phytoplankton, green, brown and red algae, sponges, cnidarians, bryozons, among others [1,2]. These natural compounds have been considered important sources for the search and development of new pharmaceuticals [3–8] and agrochemicals [9]. Besides, the chemical novelty associated with those compounds has inspired organic chemists. As a consequence, several marine natural products have been targeted for total syntheses [10–16].

The nostoclides (I) and (II) (Fig. 1) are marine natural products produced by a cyanobacterium (*Nostoc* sp.) symbiont partner within lichen *Peltigera canina*. These compounds possess a γ-benzylidene functionality and belong to the class of substances known as γ-alkylidenebutenolides [17,18].

These nostoclides displayed moderate cytotoxic effects against the mouse neuroblastoma cell lines Neuro-2aCCL and KB CCL 17 [19]. Taking into account that *P. canina* cultures are not usually contaminated with microorganisms, it has been suggested that these chlorinated compounds may be allelopathic agents.

We have been involved in the preparation and biological

* Corresponding author. Chemistry Department, Universidade Federal de Minas Gerais, CEP 3409-5720 Belo Horizonte, MG, Brazil.
** Corresponding author. Chemical Institute, Federal University of Goiás, CEP 74001-970 Goiânia, GO, Brazil.
*** Corresponding author. Institute of Chemistry, Federal University of Alfenas, CEP 37130-000 Alfenas, MG, Brazil.
E-mail addresses: lcab@ufmg.br (L.C.A. Barbosa), felipeterramartins@gmail.com (F.T. Martins), doriguetto@unifal-mg.edu.br (A.C. Doriguetto).
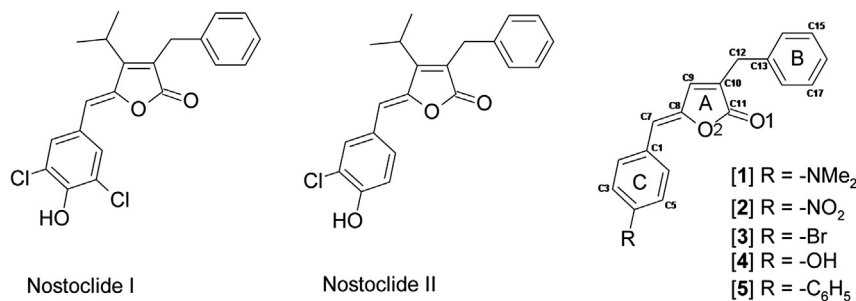
Fig. 1. Structures of nostoclides I and II and synthetic analogues [**1**–**5**] with ring and atom labeling scheme. The atom labeling of R is shown in Fig. 2.

evaluation of several nostoclide analogues [20]. It has been demonstrated that these analogues, at different degrees, are capable of interfering with photosynthetic electron transport [21–25]. In addition, we have conducted investigations on the crystal structures of nostoclide analogues [26–28]. Aiming at contributing to further understand in detail the structures of such compounds, we describe in this paper our results concerning the crystal structure of nostoclide analogues bearing benzylidene appendages functionalized at *para* position.

2. Experimental

2.1. Synthesis and preparation of crystalline samples

By using the vinylogous aldol reaction between appropriate aldehydes and furan-based silyloxydiene synthon generated from 3-benzyl-furan-2(5H)-one as the key step [29–31], compounds **1** to **5** (Fig. 2) were prepared in yields ranging from 33% to 91% [22].

The identities of nostoclide analogues **1** to **5** were confirmed upon full spectroscopic (one and two-dimensional NMR and IR) as well as mass spectrometric analyses [22]. Crystals of compounds **1**

to **5** were obtained by gently warming each compound in hexane, followed by dropwise addition of dichloromethane until the solid was completely dissolved. The resulting solution was left undisturbed at room temperature. After approximately 24 h, crystals suitable for X-ray analyses were formed. They were separated, washed with cold hexane, and dried.

2.2. Single-crystal X-ray diffraction

Prism-shaped single crystals of substances **1** to **5** were selected and mounted on the κ-goniostat of an Enraf-Nonius Kappa-CCD diffractometer. Room temperature diffraction intensities were collected using graphite-monochromated MoKα X-ray beam through φ-ω scans and κ offset [32]. The X-ray diffraction frames were recorded using the program COLLECT [33], and reduction and scaling of the raw dataset were performed with HKL Denzo-Scalepack [34].

The structures were solved by direct methods with SHELXS-97 [35]. The models were refined by the full-matrix least squares method on F^2 with SHELXL-97 [35], with anisotropic thermal parameters for non-hydrogen atoms. The hydrogen atoms were
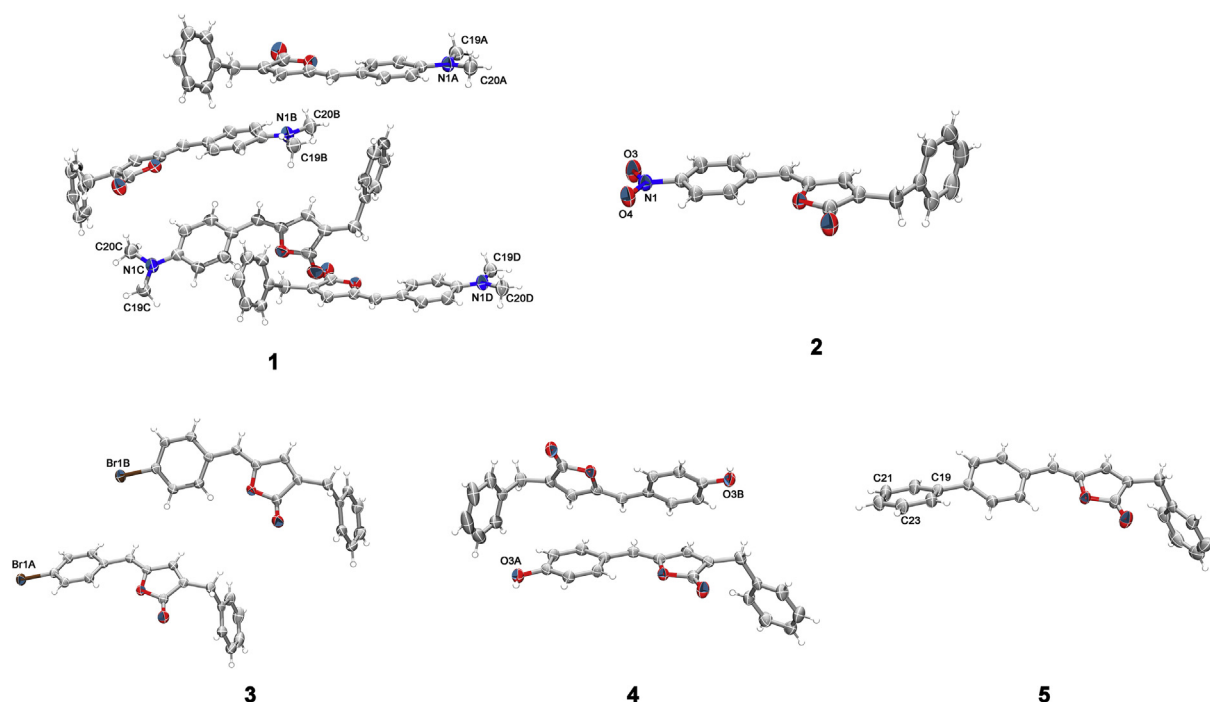

Fig. 2. ORTEP views of compounds **1** to **5** showing the atoms displacement ellipsoids at 30% probability level. Non-hydrogen atoms are arbitrarily labeled and hydrogen atoms are shown as spheres of arbitrary radii. Atom labeling scheme for nostoclide framework common to all compounds can be found in Fig. 1 ^{i} Symmetry code: x, −y + 0.5, z.

placed in idealized positions after their identification in the difference Fourier map. Then, they were refined with fixed individual isotropic displacement parameters [$U_{iso}(H) = 1.2U_{eq}$ (C_{sp}^2 or C_{sp}^3 in methylene groups) or $1.5U_{eq}$ (C_{sp}^3 in methyl groups or O)] using a riding model with bond lengths of 0.82 Å (O–H), 0.86 Å (N–H), 0.93 Å (C_{sp}^2–H), 0.97 Å (C_{sp}^3–H in methylene groups) or 0.96 Å (C_{sp}^3–H in methyl groups). A summary of crystal data and refinement statistics is given in Table 1.

The programs MERCURY [36] and ORTEP-3 [37] were used within the WinGX [38] software package to generate artworks. After the refinements had been completed, the molecular structures of all compounds were checked with MOGUL [39] tool derived from the Cambridge Structural Database (CSD [40], version 5.36 of November 2014). Crystallographic data for the structural analysis of the compounds herein discussed have been deposited at the Cambridge Crystallographic Data Centre, 12 Union Road, CambridgeCB2 1EZ, UK, and are available on request quoting the deposition numbers showed in Table 1.

3. Results and discussion

The compounds **1** to **5** are functionalized at *para* position of the C aromatic ring (see Fig. 1 for ring labeling). The exocyclic double bond of all substances presents *Z* configuration, a similar feature displayed in eight out of nine nostoclide analogues previously reported [27,28]. In addition, since analogues **1** to **5** present hydrogen atoms in the *ortho* positions of the C rings, a non-classical intramolecular hydrogen bond (C6–H6 ··· O2) is present in their structures (Fig. 2).

Compound **1** crystallizes in the non-centrosymmetric monoclinic space group P2$_1$ with four crystallographically independent molecules in its asymmetric unit (AU) as shown in Fig. 2 together with the chosen AU of the other compounds herein described. The four molecules in the AU of **1** are remarkably similar from a conformational point of view, as can be seen in Fig. 3. The highest root mean square deviation (RMSD) for the non-hydrogen atoms is
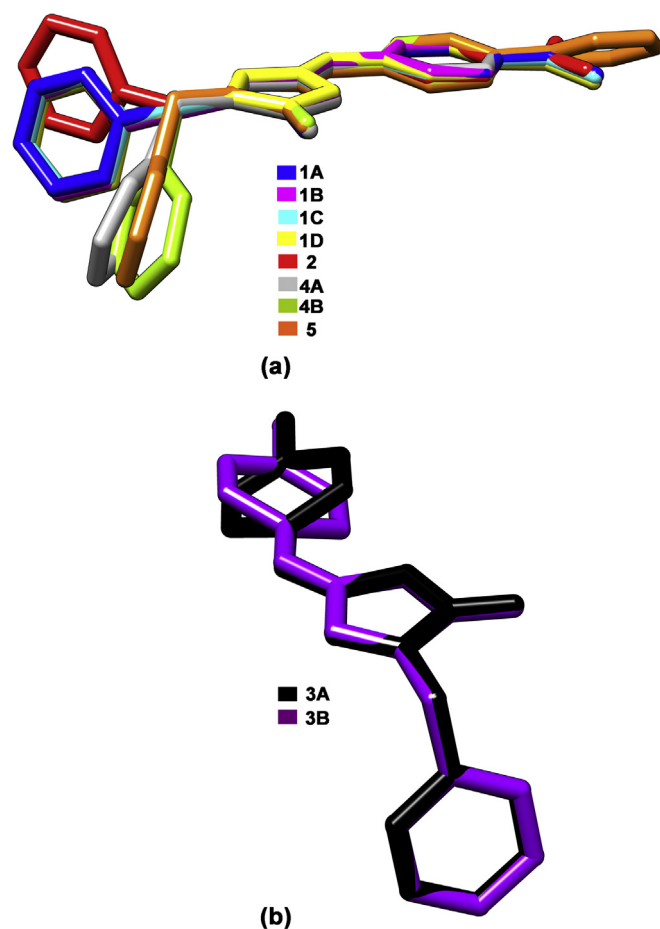
Fig. 3. Superposition of crystallographically independent molecules present with either (a) planar or (b) twisted conformation around rings A and C (see Fig. 1 for ring labeling) and neighbors.

Table 1
Crystal data and statistic refinements for compounds **1**–**5**.

		1	2	3	4	5
Structural formula		$C_{20}H_{19}N_1O_2$	$C_{18}H_{13}N_1O_4$	$C_{18}H_{13}Br_1O_2$	$C_{18}H_{14}O_3$	$C_{24}H_{18}O_2$
fw (g/mol)		305.36	307.29	341.18	278.29	338.38
Crystsyst		monoclinic	orthorhombic	monoclinic	monoclinic	monoclinic
Space group		P2$_1$	Pnma	P2$_1$/c	P2$_1$/c	P2$_1$/c
Z/Z'		8/4	4/0.5	8/2	8/2	4/1
T (K)		298(2)	298(2)	298(2)	298(2)	298(2)
Unit cell dimensions	a (Å)	18.6803(4)	22.5888(6)	17.001(3)	15.0266(4)	16.7703(7)
	b (Å)	6.39240(10)	7.0104(2)	6.0849(10)	5.74850(10)	6.4048(3)
	c (Å)	27.5903(7)	9.6324(3)	30.959(6)	35.5270(9)	16.5680(8)
	β(°)	90.5934(10)	90	113.330(8)	112.320(11)	95.147(3)
V (Å^3)		3294.44(12)	1525.35(8)	2940.8(9)	2838.9(3)	1772.40(14)
Calculated density (Mg/m^3)		1.231	1.338	1.541	1.302	1.268
Absorption coefficient μ (mm^{-1})		0.079	0.096	2.797	0.088	0.079
θ range for data collection (°)		2.95–25.35	3.42–25.34	3.02–25.65	2.93–25.37	3.31–26.71
Index ranges	h	−22 to 22	−27 to 27	−20 to 18	−18 to 18	−21 to 21
	k	−7 to 7	−8 to 8	−7 to 7	−6 to 6	−6 to 8
	l	−32 to 33	−11 to 11	−37 to 37	−42 to 42	−20 to 20
data collected		37752	9773	45993	25909	15878
unique reflections		11762	1498	5552	5153	3704
Symmetry factor (R_{int})		0.1029	0.0444	0.0894	0.1009	0.0821
Completeness to $θ_{max}$ (%)		99.2	98.5	99.5	99.2	98.5
F (000)		1296	640	1376	1168	712
parameters refined		837	135	379	381	235
Goodness-of-fit on F^2		1.033	1.033	1.011	0.927	1.008
Final *R1*factor for $I > 2σ(I)$		0.0541	0.0475	0.0342	0.0432	0.0512
wR2 factor for all data		0.1467	0.1403	0.0842	0.1148	0.1595
Largest diff. peak/hole (e/Å^3)		0.220/−0.253	0.118/−0.163	0.242/−0.320	0.131/−0.131	0.249/−0.214
CCDC deposit number		1402321	1402322	1402323	1402324	1402325

0.1509 Å when overlapping molecules **1A** to **1D** (largest atom deviation of 0.2671 Å for C16). Their conformations are almost completely planar, except for the benzyl moiety (B ring attached to the methylene group according to labeling scheme shown in Fig. 1) twisted by 76.16(8)°, 76.94(8)°, 78.70(9)° and 79.44(8)° in molecules **1A**, **1B**, **1C** and **1D**, respectively, from the least-square plane calculated through the non-hydrogen atoms of rings A and C (including carbonyl oxygen) and C7. This averaged plane will be hereinafter referred as the molecular mean plane of nostoclide analogues. The RMSD of the thirteen fitted atoms onto the molecular mean plane was 0.0377 Å, 0.0555 Å, 0.0320 Å, 0.0479 Å in molecules **1A1B**, **1C** and **1D**, respectively, with largest atom deviation of 0.0618 Å (C6), 0.0837 Å (C4), 0.0513 Å (C6) and 0.0658 Å (C4), respectively.

The planarity of the ring system involving rings A and C (see Fig. 1 for labeling) can also be associated with the torsional angle C8–C7–C1–C2 (see Table 2) in terms of deviation from 180 or 0°, as discussed in our more recent published article on nostoclide analogues [25]. The N,N-dimethylamino group is coplanar with phenyl ring C, as observed in the torsions on the N1–C4 bond axis measuring close to either 0° or 180° (Table 2). Thus, this group acts as a π-electron-donating substituent. This phenomenon can be also observed in the C–N–C valence angles close to 120° revealing the sp^2-hybridization of nitrogen (Table 2). In fact, the delocalized resonance seems to be extended over the ring A up to the neighboring unsaturated carbon, i. e., the C_{sp}^2-C_{Ar} bond length is shorter than an expected single-bond distance (this mean value is 1.441(5) Å in compound **1** against 1.47(2) Å, the mean value averaged on 3972 structures deposited in the CSD. This shortening of bond length was also observed for all compounds of the series as consequence of their conjugated para-substituent (Table 2). In addition, the conformation of benzyl moiety is the main responsible for crystallization of compound **1** in the chiral space group P2₁. Taking the molecular mean plane crossing through rings A and C and their neighbors as a reference, phenyl ring B lies on the opposite side of lactone oxygens. However, in this structure none of the molecules can be related by mirror symmetry. If they could be

related by such symmetry element, the mirror molecules would differ conformationally from those found in the crystal structure reported here by a rotation of 60° towards the nostoclide mean plane on the bond axis between the α-carbon and the methylene one (C10–C12. In other words, there is only one of the two conformations with phenyl ring C at the equatorial position opposite to the lactone oxygen either above or below the molecular mean plane. Unfortunately, the absolute configuration could not be determined from X-ray crystallographic analysis. This was not possible due to the fact that the most electron-rich atom (O) does not have a large enough anomalous scattering (using MoKα radiation) to allow the determination of reliable Flack parameter with standard uncertainty lower than the safe upper limit of 0.10.

Compound **2**, containing a para-nitro functionality instead of the N,N-dimethylamino group of compound **1**, crystallizes with a half of one molecule in the asymmetric unit (Fig. 2). This is due to the location of one molecule on a symmetry element present in the centrosymmetric orthorhombic space group Pnma. Except for phenyl ring B, compound **2** is completely planar with all atoms (including methylene carbon C12 and those of phenyl ring B labeled as C13 and C16) sitting on a mirror plane at (y,½, z). In fact, only four atoms are outside the m mirror plane normal to b crystallographic axis and passing through the remaining atoms (C14, C14ⁱ, C15, and C15ⁱ). Consequently, these four atoms are normal to the m mirror plane and the phenyl ring B is also oriented towards opposite side of lactone oxygen in compound **2**, forming an angle of 90.00(5)° with the molecular plane. Because of these geometric features, compounds **1** and **2** are, therefore, conformationally similar in terms of the planar fragment formed by the rings A and C and the twist angle of the phenyl ring B in relation to the lactone oxygen present in the planar moiety (Fig. 3). However, compounds **1** and **2** do slightly differ in terms of a rotation on the bond axis between the C10 α-carbon and C12 methylene atoms (Fig. 3). While the syn torsional angle around this bond axis is 0° in compound **2**, this value is 25.5(7)° on average in compound **1** (Table 2).

Brominated compound **3** presents some similarities to compounds **1** and **2** (Fig. 2). However, the presence of the bromine

Table 2
Selected bond lengths (Å), valence and torsion angles (°) for compounds **1–5**.

Parameter	1A	1B	1C	1D	2	3A	3B	4A	4B	5
O1–C11	1.198(4)	1.199(3)	1.200(4)	1.198(3)	1.197(3)	1.194(3)	1.194(3)	1.208(2)	1.210(2)	1.200(2)
O2–C11	1.383(4)	1.380(3)	1.382(4)	1.386(4)	1.387(3)	1.395(3)	1.398(3)	1.379(2)	1.380(2)	1.386(2)
O2–C8	1.392(3)	1.389(3)	1.393(3)	1.392(3)	1.376(3)	1.385(3)	1.389(3)	1.393(2)	1.399(2)	1.3846(19)
Xᵃ–C4	1.372(4)	1.379(4)	1.366(4)	1.366(4)	1.465(3)	1.897(2)	1.896(2)	1.362(2)	1.358(2)	1.493(2)
C1–C7	1.443(4)	1.444(4)	1.445(4)	1.433(4)	1.449(3)	1.464(3)	1.457(3)	1.448(2)	1.452(2)	1.450(2)
C7–C8	1.344(4)	1.340(4)	1.341(4)	1.341(4)	1.337(3)	1.338(3)	1.330(3)	1.337(2)	1.329(2)	1.334(2)
C8–C9	1.428(4)	1.431(4)	1.434(4)	1.422(4)	1.448(3)	1.439(3)	1.441(3)	1.436(2)	1.429(2)	1.439(2)
C9–C10	1.331(4)	1.327(4)	1.338(4)	1.336(4)	1.325(3)	1.331(3)	1.330(3)	1.334(2)	1.335(3)	1.331(2)
C10–C11	1.454(4)	1.445(4)	1.454(4)	1.443(4)	1.466(3)	1.465(4)	1.468(3)	1.460(3)	1.456(3)	1.455(2)
C4–N1–C19	122.3(3)	121.2(3)	121.7(3)	121.3(3)	–	–	–	–	–	–
C4–N1–C20	120.2(3)	120.3(3)	120.8(3)	121.1(3)	–	–	–	–	–	–
C19–N1–C20	116.2(3)	117.8(3)	117.1(3)	117.3(3)	–	–	–	–	–	–
C2–C1–C7–C8	176.1(3)	177.1(3)	177.8(3)	177.6(3)	180	162.6(3)	−166.3(3)	175.63(19)	−175.79(19)	−171.90(18)
C6–C1–C7–C8	−1.4(5)	−0.4(5)	−1.5(5)	0.0(5)	0	−16.9(4)	17.7(4)	−3.8(3)	3.8(3)	7.3(3)
C3–C4–N1–C19	−172.6(3)	−175.1(3)	−174.4(3)	−176.4(3)	–	–	–	–	–	–
C3–C4–N1–C20	−5.8(4)	−4.7(4)	−2.2(4)	−3.4(5)	–	–	–	–	–	–
C5–C4–N1–C19	8.3(4)	5.3(4)	5.2(4)	4.2(5)	–	–	–	–	–	–
C5–C4–N1–C20	175.0(3)	175.7(3)	177.4(3)	177.3(3)	–	–	–	–	–	–
C9–C10–C12–C13	25.0(5)	24.9(5)	26.4(5)	25.7(5)	0	91.3(3)	96.8(3)	103.9(2)	109.2(2)	113.5(2)
C11–C10–C12–C13	−155.3(3)	−155.1(3)	−154.2(3)	−153.2(3)	180	−83.7(3)	−80.5(3)	−79.9(2)	−70.9(2)	−66.8(2)
C10–C12–C13–C14	92.5(3)	95.7(4)	91.3(3)	93.4(3)	88.95(19)	95.0(3)	94.6(3)	134.2(2)	89.6(2)	116.8(2)
C10–C12–C13–C18ᵇ	−88.1(4)	−85.6(4)	−89.2(4)	−86.7(4)	−88.95(19)	−83.5(3)	−84.0(3)	−49.0(3)	−89.6(2)	−63.9(2)

ᵃ X is N1 in compounds 1 and 2, Br1 in compound 3, O3 in compound 4 and C19 in compound 5.
ᵇ In compound 2, C18 is the mirror image of C14 reflected through the mirror plane at (y,½, z).

results in some conformational changes when compared to the *N,N*-dimethylamino and nitro analogues. Compound **3** crystallizes in the centrosymmetric monoclinic space group P2$_1$/*c* with two molecules in the asymmetric unit (Fig 2). While rings A and C and neighbors are coplanar in **1** and **2**, there is a twisting into this molecular backbone in both crystallographically independent molecules of compound **3**. Rings A and C form an angle of 19.46(7)° and 22.57(7)° in molecules **3A** and **3B** as a consequence of rotation on the single bond axis between them (see also torsional angle C8−C7−C1−C2 in Table 2). Although these rotations have similar degree values in the two conformers, they occur toward opposite sides of lactone plane (Fig. 3), as can be seen by the similar values of the torsions on the C1−C7 bond axis but with opposite signs (Table 2). These opposite signs are observed when measuring torsions are made on the same enantiomorphs of the conformers, *i. e.*, taken into account if phenyl ring B is in the axial position of bonding to methylene carbon on the same side of the lactone mean plane. Identical enantiomorphs were chosen as asymmetric units for this compound. One can also note that axial position of this ring in compound **3** differs from an equatorial one found in compound **1** (Fig. 3). Furthermore, ring B is almost perpendicular to lactone mean plane such as in the other two compounds, having an angle between them of 74.55(9)° and 74.87(8)° in molecules **3A** and **3B**.

A similar benzyl conformation is also observed for compounds **4** and **5**, which have a hydroxyl and phenyl group at *para*-position of ring C, respectively. In compound **4**, there are two conformers in its asymmetric unit (space group P2$_1$/*c*) with a planar molecular backbone resembling that of compounds **1** and **2** and phenyl ring B at axial position such as compound **3** (Fig. 3). The RMSD of the thirteen fitted atoms onto the molecular mean plane was 0.0549 Å and 0.0663 Å in molecules **4A** and **4B**, with largest atom deviation of 0.106 Å (C6) and 0.102 Å (C3), respectively. This mean plane forms an angle of 72.05(5)° and 68.38(6)° with phenyl ring B in these molecules (see also the torsional angle C8−C7−C1−C2 in Table 2). Nevertheless, these molecules of **4** are not superimposable due to rotation on the single bond axis into benzyl group changing the conformation of the phenyl head (see torsion values in Table 2 around the C12−C13bond between methylene and phenyl carbons).

The molecular backbone of the single molecule in the asymmetric unit of compound **5** is also planar, albeit not as planar as noticed for compounds **1**, **2** and **4**. The RMSD of **5** for its non-hydrogen atoms of the molecular mean plane (0.0901 Å, largest deviation of 0.139 Å for C3) is higher than RMSD values aforementioned for analogues **1**, **2**, **4**. Moreover, the molecular mean plane of **5** and ring B are twisted by 76.74(5)°, similarly to all other
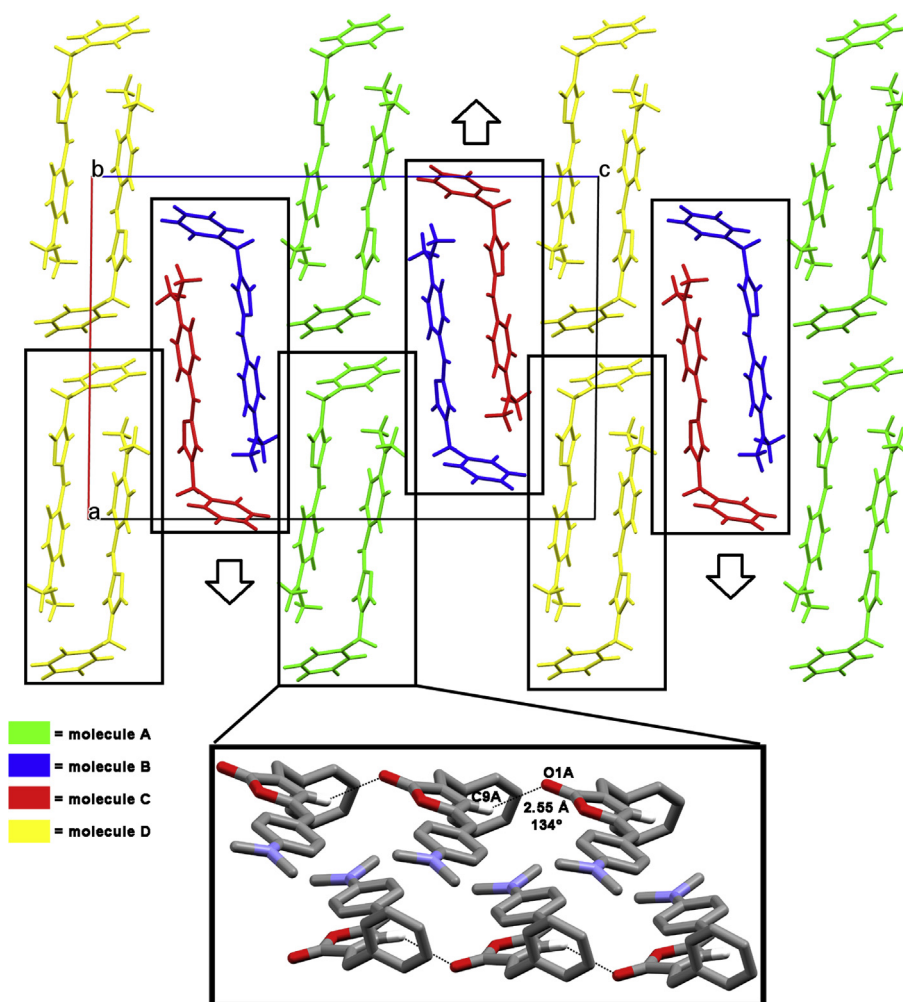

Fig. 4. The crystal packing of compound **1**. Arrows detach the displacement of BC double catemers along the [100] direction when packed through c-axis (observe the translation symmetry equivalence between framed AA and DD double chains). An AA double catemer running along the [010] direction is highlighted in the bottom frame. In this picture and in most following illustrations, only hydrogen atoms involved in hydrogen bonds are shown. In this picture and in all following ones, only non-hydrogen atoms involved showing intermolecular contacts are labeled as well as the displayed measurements refer to hydrogen … acceptor atom (or C_g) distance and hydrogen bonding angle.
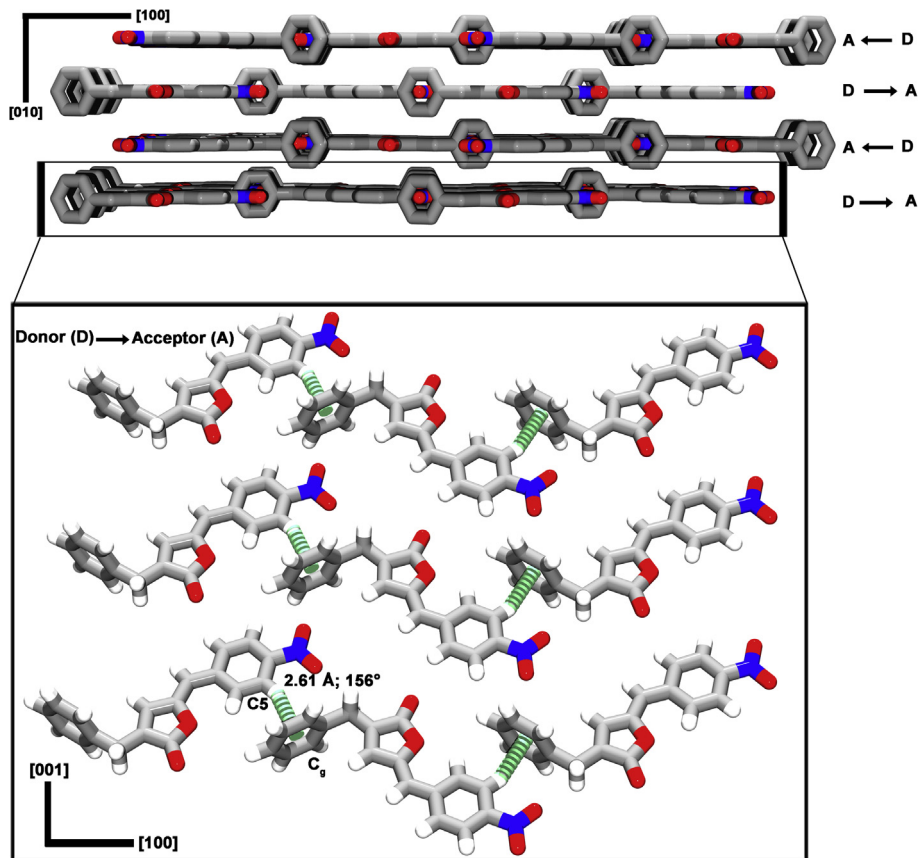
Fig. 5. The layered structure of compound **2**. The term C_g does refer to centroid calculated through the phenyl ring C carbons.
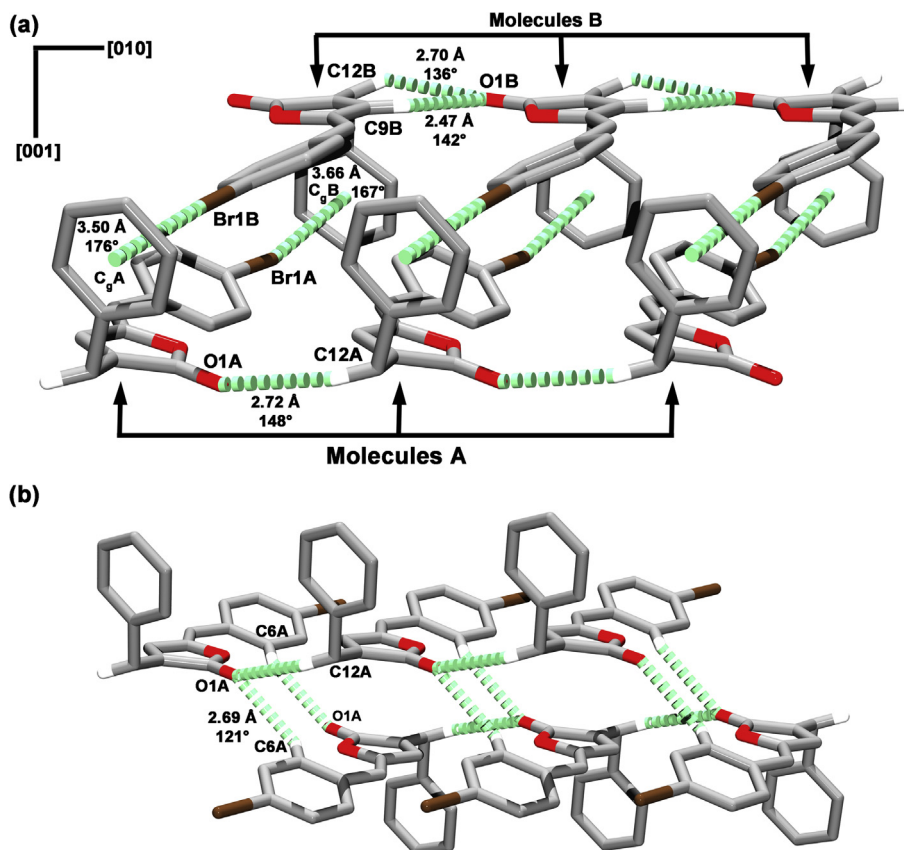

Fig. 6. (a) The double catemers of **3** are connected through halogen … π interactions. The terms C_gA and C_gB refer to centroids calculated through the phenyl ring C carbons from molecules A and B, respectively. (b) Neighboring chains composed by molecules B are interacting through weak non-classical hydrogen bonds.

analogues (see also the torsional angle C8−C7−C1−C2 in Table 2). Finally, phenyl rings in the biphenyl moiety are bent by 35.21(6)°.

The crystal packing of compound **1** is stabilized through formation of chains assembled parallel to the [010] direction through C−H ··· O=C nonclassical hydrogen bonds between lactone moieties from translation-symmetry related molecules (Fig. 4). Therefore, these catemers are composed by a same crystallographically independent molecule. Each chain made up of molecules A and D is face-to-face stacked on top of one another assembled with the same crystallographically independent molecule giving rise to AA and DD double catemer motif. On the other hand, each chain of molecules B is face-to-face stacked on top of one catemer composed by molecules C (BC double catemer). There are stacking angles of 33.13(5)°, 33.18(6)° and 32.98(5)° between the molecular mean planes into the AA, DD and BC double chains, respectively. The double chains of molecules A or D are related by translation symmetry along the *c* axis (Fig. 4). However, their packing along this axis is intercalated by BC double catemer, which are displaced along the *a*-axis when distributed over the *c*-axis. If they were not displaced parallel to the [100] direction, the *c*-axis length would be half of the current one as consequence of translation-symmetry equivalence between AA and DD double catemers and between BC double chains themselves.

Crystal packing of compound **2** is marked by the presence of layers assembled with face-to-edge C−H ··· π contact between rings A and C (Fig. 5). This interaction gives rise to infinite one-dimensional zigzag chains running along the [100] direction. In addition, the molecular layers are stacked along the [010] direction with stacking distances of 3.5 Å. Neighboring layers have their catemers growing in opposite directions as shown in top panel of Fig. 5.

The conformerism observed in compound **3** can be explained from crystal packing inspection (Fig. 6). In this structure, there are catemers made up of only one conformer growing along the [010] direction. These chains are face-to-face stacked to allow the formation of halogen … π interactions between *para*-bromine atom and ring C. However, the assembly of the chains differs slightly. In the catemer formed by molecules B, lactone mean planes are more aligned than in the chains composed of molecules A. These least−square planes are separated by 1.277(18) Å and 0.121(17) Å in the chains of molecules A and B, respectively. Such higher alignment in molecule B catemers is due to bifurcated non-classical C−H ··· O hydrogen bond setting in-plane both lactone and methylene C−H donor groups from the same molecule and carbonyl oxygen from a neighbor one. Besides interacting with methylene group in the molecule A chain, this oxygen atom is also an acceptor from
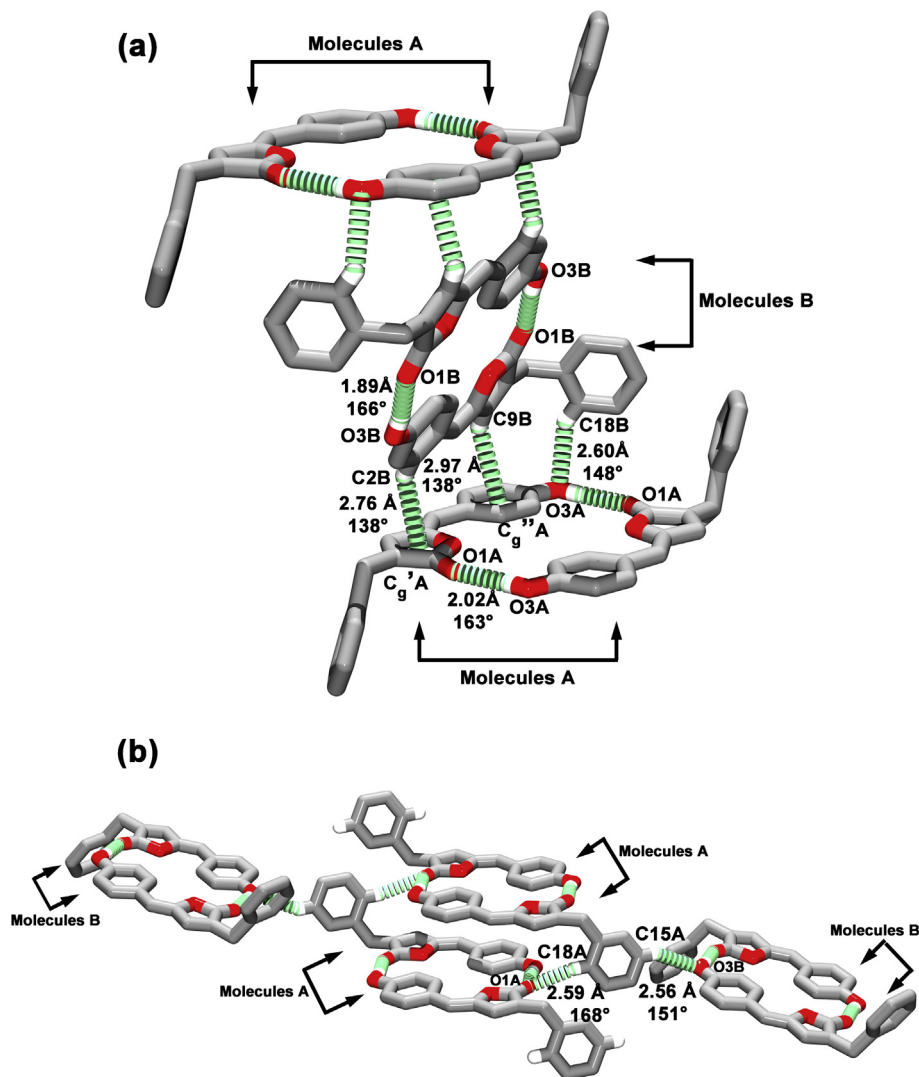

Fig. 7. (a) The centrosymmetric dimers of **4**. The terms $C_g'A$ and $C_g''A$ do refer to centroids calculated through the carbons of phenyl rings B and A from molecule A. (b) The non-classical hydrogen bonds involving the phenyl ring C of molecule A.
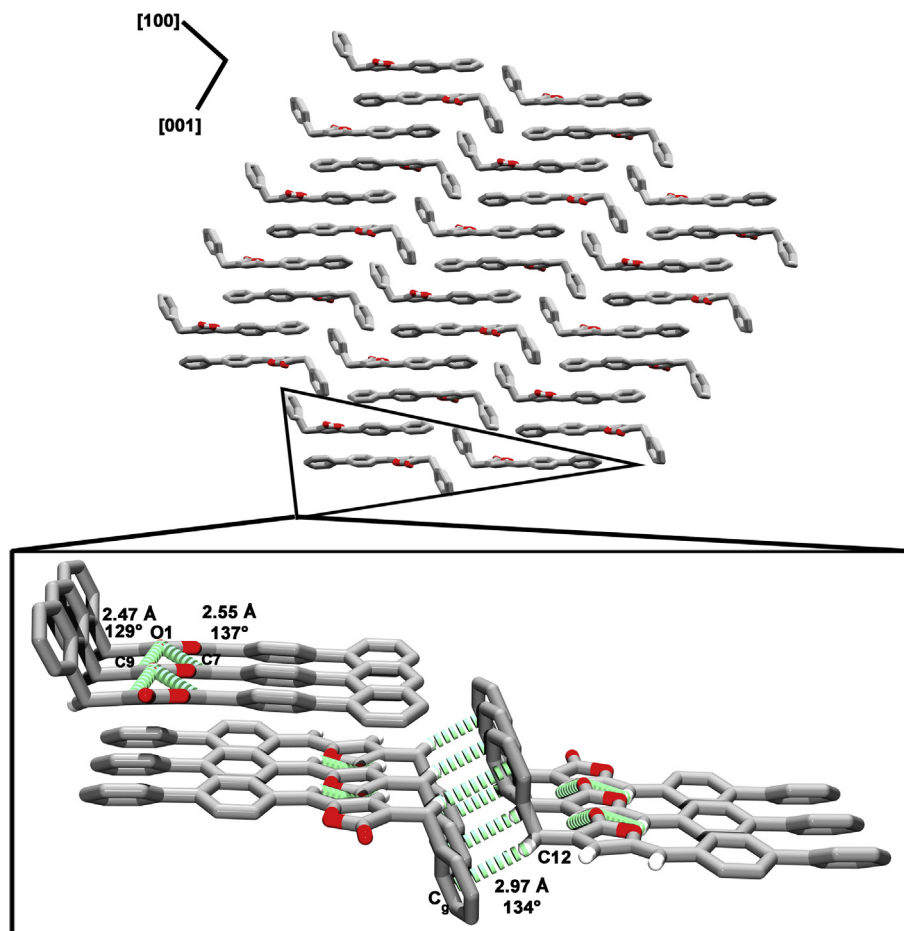
Fig. 8. The crystal packing of **5**. Catemers running along the [010] direction are detached in the bottom frame. The term C_g refers to centroid calculated through the phenyl ring C carbons.

phenyl C—H moiety from another molecule A stacked on a neighboring catemer (Fig. 6).

Compound **4** is the only nostoclide derivative herein described presenting classical intermolecular hydrogen bonds, namely the O—H … O=C interaction between *para*-hydroxyl and carbonyl groups. Again, this interaction occurs between molecules of the same conformation, giving rise to centrosymmetric dimers AA or BB (Fig. 7). These dimers are connected through face-to-edge C—H ⋯ π interactions in which lactone (C9—H9) and phenyl ring A (C2—H2) from molecule B are donors to phenyl rings A and B from molecule A. In these interactions, the molecular mean planes form an angle of 63.61(3)°. In this structure, the pattern of weak non-classical hydrogen bonds helps to understand the observed conformerism. Phenyl ring C from molecule A is twisted to interact simultaneously as a C—H hydrogen bonding donor to carbonyl and hydroxyl oxygen atoms from neighboring molecules A and B (Fig. 7b), respectively, while this phenyl ring from molecule B donates only one hydrogen bonding to hydroxyl oxygen from molecule A (Fig. 7a).

It is noteworthy to mention the role of lactone carbonyl O1 oxygen in the crystal packing of nostoclide analogues. It participates as a bifurcated non-classical hydrogen bonding acceptor in the structure of compound **5**, being responsible to assemble chains parallel to [010] direction together with olefin C—H moieties from lactone (C9—H9) and the unsaturated bridge (C7—H7) as depicted in the frame highlighted in Fig. 8.

These catemers are stacked along the [−101] direction, with a stacking angle between the molecular mean planes of 24.62(3)°. Furthermore, there is C—H … π contacts between methylene group

and phenyl ring C parallel to the [101] completing the three-dimensional packing (Fig. 8).

4. Conclusion

We have here prepared five new nostoclides analogues and their crystal structures were elucidated. Three compounds exhibit a $Z' > 1$ value as a result of either conformerism (compounds **3** and **4**, $Z' = 2$) or absence of intermolecular symmetry into the asymmetric unit (compound **1**, $Z' = 4$). In the last case, the four crystallographically independent molecules adopt the same conformation while their C—H … O=C nonclassical hydrogen bonded double catemers are offset packed. Also in the crystal structure of compound **1**, there is only one of the two mirror conformations with phenyl ring B at the equatorial position opposite to the lactone oxygens either above or below the molecular mean plane. This behavior is responsible for its crystallization in the chiral space group P2₁ even though this molecule does not have a stereocenter. The molecular mean plane of nostoclide analogues have been featured by high level of planarity, except in compound **3** that is present in two twisted conformations arising from rotations on the single bond axis between lactone and phenyl rings. Even complete planarity of the molecular backbone onto a mirror plane was observed in compound **2**. Moreover, the main conformational variability among the compounds studied here is in the benzyl moiety. For instance, the benzyl conformation has been the greatest difference between the two crystallographically independent molecules of compound **4**. In their crystal packing, there is

formation of −H … O=C nonclassical hydrogen bonded double chains in compounds **1**, **3** and **5**. Therefore, this double catemer motif is the main supramolecular way to pack nostoclides, although C−H … π interactions do play an important assembly role in the crystal packing of compounds **2** and **5**. At last, we believe this study will contribute to a better understanding of how substitution pattern does affect the conformation and intermolecular array of nostoclides, besides furnishing their structural knowledge in full detail.

Conflict of interest

The authors declare that they have no conflict of interest.

Acknowledgments

References

[1] J.N. Blunt, B.R. Copp, R.A. Keyzers, M.H.G. Munro, M.R. Prinsep, Nat. Prod. Rep. 32 (2015) 116−211.
[2] D.A. Dias, S. Urban, U. Roessner, Metabolites 2 (2012) 303−336.
[3] Y. Liu, J. Marine, Sci. Res. Dev. 2 (2012) 1−2.
[4] R. Montaser, H. Luesch, Future Med. Chem. 3 (2011) 1475−1489.
[5] A.M.S. Mayer, K.B. Glaser, C. Cuevas, R.S. Jacobs, W. Kem, R.D. Little, J.M. McIntosh, D.J. Newman, B.C. Potts, D.E. Shuster, Trends Pharmacol. Sci. 31 (2010) 255−265.
[6] K.B. Glaser, A.M.S. Mayer, Biochem. Pharmacol. 78 (2009) 440−448.
[7] E. Marris, Nature 443 (2006) 904−905.
[8] B. Haefner, Drug Discov. Today 8 (2003) 536−544.
[9] J. Peng, X. Shen, K.A. El Sayed, D.C. Dunbar, T.L. Perry, S.P. Wikins, M.T. Hamann, S. Bobzin, J. Huesing, R. Camp, M. Prinsen, D. Krupa, M.A. Wideman, J. Agric. Food Chem. 51 (2003) 2246−2252.
[10] S. Boucle, C. Melin, M. Clastre, J. Guilard, Mar. Drugs 13 (2015) 655−665.
[11] M. Sasaki, H. Fuwa, Chem. Rec. 14 (2014) 678−703.
[12] Z.-Y. Yang, H.-Z. Liao, K. Sheng, Y.-F. Chen, Z.-J. Yao, Angew. Chem. Int. Ed. 51 (2012) 6484−6487.
[13] T. Kuranaga, N. Ohtani, R. Tsutsumi, D.G. Baden, J.L.C. Wright, M. Satake, K. Tachibana, Org. Lett. 13 (2011) 696−699.
[14] P.S. Baran, T.J. Maimone, J.M. Richter, Nature 22 (2007) 404−408.
[15] M. Sasaki, H. Fuwa, M. Ishikawa, K. Tachibana, Org. Lett. 1 (1999) 1075−1077.
[16] D.W.C. MacMillan, L.E. Overman, J. Am. Chem. Soc. 117 (1995) 10391−10392.
[17] L.C.A. Barbosa, R.R. Teixeira, G.W. Amarante, Curr. Org. Synth. 12 (2015) 746−771.
[18] L.C.A. Barbosa, R.R. Teixeira, P.F. Pinheiro, C.R.A. Maltha, A.J. Demuner, Quim. Nova 33 (2010) 1163−1174.
[19] X. Yang, Y. Shimizu, J.R. Steiner, J. Clardy, Tetrahedron Lett. 34 (1993) 761−764.
[20] J. Boukouvalas, F. Maltais, N. Lachance, Tetrahedron Lett. 35 (1994) 7897−7900.
[21] L.C.A. Barbosa, M.E. Rocha, R.R. Teixeira, C.R.A. Maltha, G. Forlani, J. Agric. Food Chem. 55 (2007) 8562−8569.
[22] R.R. Teixeira, L.C.A. Barbosa, G. Forlani, D.P. Veloso, J.W.M. Carneiro, J. Agric. Food. Chem. 56 (2008) 2321−2329.
[23] L.C.A. Barbosa, A.J. Demuner, C.R.A. Maltha, R.R. Teixeira, K.A.P. Souza, K.U. Bicalho, Z. Naturforsch 64b (2009) 245−251.
[24] L.C.A. Barbosa, J.O.S. Varejão, D. Petrollino, P.F. Pinheiro, A.J. Demuner, C.R.A. Maltha, G. Forlani, Arkivoc iv (2012) 15−32.
[25] R.R. Teixeira, P.F. Pinheiro, L.C.A. Barbosa, J.W. Carneiro, G. Forlani, Pest. Manag. Sci. 66 (2010) 196−202.
[26] R.R. Teixeira, L.C.A. Barbosa, J.O.S. Varejão, D.P. Veloso, J. Ellena, A.C. Doriguetto, M.G.B. Drew, F.M.D. Ismail, J. Mol. Struct. 837 (2007) 197−205.
[27] R.R. Teixeira, L.C.A. Barbosa, J.W.M. Carneiro, R.S. Corrêa, J. Ellena, A.C. Doriguetto, J. Mol. Struct. 917 (2009) 1−9.
[28] R.R. Texeira, L.C.A. Barbosa, M.A. Kabeshov, C.R.A. Maltha, R.S. Corrêa, A.C. Doriguetto, J. Mol. Struct. 1075 (2014) 53−62.
[29] X. Jusseau, L. Chabaud, C. Guilou, Tetrahedron 70 (2014) 2595−2615.
[30] G. Casiraghi, L. Battistini, C. Curti, G. Rassu, F. Zanardi, Chem. Rev. 111 (2011) 3076−3154.
[31] C.W. Jefford, D. Jaggi, J. Boukouvalas, Tetrahedron Lett. 28 (1987) 4037−4040.
[32] Bruker -Nonius, Kappa CCD Reference Manual, 1998. Nonius B.V., P.O. Box 811, 2600 Av, Delft, The Netherlands.
[33] Nonius, COLLECT. Nonius BV, Delft, The Netherlands, 1999.
[34] Z. Otwinowski, W. Minor, in: C.W. Carter Jr., R.M. Sweet (Eds.), Methods in Enzymology, Macromolecular Crystallography Part a, vol. 276, Academic Press, New York, 1997, pp. 307−326.
[35] G.M. Sheldrick, Acta Cryst. A64 (2008) 112−122.
[36] P.R. Edgington, P. McCabe, C.F. Macrae, E. Pidcock, G.P. Shields, R. Taylor, M. Towler, J. van de Streek, J. Appl. Cryst. 39 (2006) 453−457.
[37] L.J. Farrugia, J. Appl. Cryst. 30 (1997) 565.
[38] L.J. Farrugia, J. Appl. Cryst. 32 (1999) 837−838.
[39] I.J. Bruno, J.C. Cole, M. Kessler, J. Luo, W.D.S. Motherwell, L.H. Purkis, B.R. Smith, R. Taylor, R.I. Cooper, S.E. Harris, A.G. Orpen, J. Chem. Inf. Comput. Sci. 44 (2004) 2133−2144.
[40] F.H. Allen, Acta Cryst. B58 (2002) 380−388.